

Historical Progress of Stereotactic Radiation Surgery

Navid Khaledi¹, Rao Khan^{2,3}, James L. Gräfe^{2,4}

¹Department of Medical Physics, Cancer Care Manitoba, Winnipeg, MB, ²Department of Physics, Toronto Metropolitan University, Toronto, ON, Canada, ³Department of Physics and Astronomy and Department of Radiation Oncology, Howard University, Washington, District of Columbia, USA, ⁴Cancer Care Program, Dr. H. Bliss Murphy Cancer Center, 300 Prince Philip Drive St. John's, NL, Canada

Abstract

Radiosurgery and stereotactic radiotherapy have established themselves as precise and accurate areas of radiation oncology for the treatment of brain and extracranial lesions. Along with the evolution of other methods of radiotherapy, this type of treatment has been associated with significant advances in terms of a variety of modalities and techniques to improve the accuracy and efficacy of treatment. This paper provides a comprehensive overview of the progress in stereotactic radiosurgery (SRS) over several decades, and includes a review of various articles and research papers, commencing with the emergence of stereotactic techniques in radiotherapy. Key clinical aspects of SRS, such as fixation methods, radiobiology considerations, quality assurance practices, and treatment planning strategies, are presented. In addition, the review highlights the technological advancements in treatment modalities, encompassing the transition from cobalt-based systems to linear accelerator-based modalities. By addressing these topics, this study aims to offer insights into the advancements that have shaped the field of SRS, that have ultimately enhanced the accuracy and effectiveness of treatment.

Keywords: Artificial intelligence, cyberknife, gamma knife, history, radiosurgery, stereotactic body radiation therapy, stereotactic radiosurgery, stereotactic radiotherapy, Zap-X, radiotherapy

Received on: 04-05-2023

Review completed on: 24-09-2023

Accepted on: 27-09-2023

Published on: 05-12-2023

INTRODUCTION

Stereotaxy is a method for localizing and accessing brain structure for removing lesions or recording electroencephalogram through surgery and related immobilization head frames. The first efforts were made in 1908 by Sir Horsley and Clarke in the UK on a monkey brain.^[1] Later, this approach became a common procedure in the surgery of the human brain. Inspired by this technique and the use of its fixation equipment, as well as the replacement of surgical instruments with ionizing radiation, an alternative method called stereotactic radiosurgery (SRS) was developed.

Stereotactic radiation therapy, as a subset of radiation therapy, aims to deliver a high dose per treatment fraction in a limited number of sessions to a regional tumor. This method may be used for the treatment of the brain or other sites of the body. Depending on the number of fractions, treated site, and size of the tumor, different modalities and techniques are employed. The term “stereotactic radiosurgery” (SRS) refers to a single (or two) fraction (s) of 18–25 Gy dose delivered to brain lesions.^[2,3] On the other hand, when the number of fractions is

increased up to 5 fractions,^[3] the dose per fraction is decreased and this technique is called “stereotactic radiotherapy” (SRT) or fractionated SRT (FSRT), which is usually used for larger tumors.^[4] Furthermore, 2–5 fraction hypofractionated SRS may also be used in some cases to maintain tumor control with less normal tissue complications.^[5] For tumors outside the cranium, such as liver, lung, bone, and prostate, the treatment is referred to as stereotactic body radiation therapy (SBRT) or stereotactic ablative radiotherapy which delivers 30–60 Gy in 1–12 fractions.^[2]

The major advantages of radiosurgery over surgery are its noninvasiveness, its ability to spare critical areas such as the brainstem, and its treatment of multiple tumors.^[3] In addition, the probability of local recurrence in SRS-only for some brain tumors is lower than in surgery alone.^[6] All of these alongside lower side effects increase the patient’s quality of life. In

Address for correspondence: Dr. Navid Khaledi,
Department of Medical Physics, Cancer Care Manitoba,
Winnipeg, MB, Canada.
E-mail: navid.khaledi@ryerson.ca

Access this article online

Quick Response Code:



Website:
www.jmp.org.in

DOI:
10.4103/jmp.jmp_62_23

This is an open access journal, and articles are distributed under the terms of the Creative Commons Attribution-NonCommercial-ShareAlike 4.0 License, which allows others to remix, tweak, and build upon the work non-commercially, as long as appropriate credit is given and the new creations are licensed under the identical terms.

For reprints contact: WKHLRPMedknow_reprints@wolterskluwer.com

How to cite this article: Khaledi N, Khan R, Gräfe JL. Historical progress of stereotactic radiation surgery. J Med Phys 2023;48:312-27.

addition, compared to whole brain radiation therapy, the patient experiences lower side effects.^[7] The treatment duration is also much shorter than conventional radiation treatments, which may take 2–3 weeks.

In recent years, significant advancements have been made in the field of SRS and SBRT. These noninvasive techniques offer precise and highly targeted treatment options for patients with various cranial and extracranial lesions. The emergence of SRS and SBRT has been driven by developments in technology, imaging modalities, treatment delivery systems, and an improved understanding of radiobiology. These advances have transformed the landscape of radiation therapy, providing patients with a more comfortable and efficient treatment experience while maintaining or even enhancing treatment efficacy. Furthermore, organizations such as the American Association of Physicists in Medicine (AAPM) have played a crucial role in shaping the guidelines and protocols for SRS and SBRT, with Task Group 178^[8] providing comprehensive recommendations to ensure the safe and effective implementation of these techniques.

More than half a century has passed since the advent of SRS.^[9] In this period, several SRS and SRT techniques and modalities such as Gamma Knife (GK),^[10] Cyberknife,^[11] VERO,^[12] Zap-X,^[13] as well as linear accelerator (Linac)-based treatments have been developed. In this review, we will mainly focus on the treatment of cranial lesions by stereotactic techniques, and discuss the history, background, technical, technological, and clinical fundamentals and challenges of SRS and SRT.

HISTORY OF STEREOTACTIC RADIOSURGERY AND STEREOTACTIC RADIOTHERAPY

Radiosurgery is often associated with the neurosurgeon Lars Leksell, who invented the first generation of GK in 1968.^[14] He initially employed an X-ray tube operating in the orthovoltage energy range. Eventually, using 179 cobalt-60 sources, along with his physicist colleague Borje Larsson, he was able to treat the first patients with this device. The 179 cobalt sources were located on a hemisphere helmet, all of them aimed toward a focal point of the hemisphere. The patients were set up in such a way that the tumor was placed at the focal spot of the irradiation. The result of the cumulative effect of gamma rays from different directions caused a high dose in the tumor and reduced the radiation dose in the surrounding normal tissues. Figure 1 shows one of the first GK units sold by Scanditronix (Scanditronix AB, Uppsala, Sweden) in 1983. Due to the lack of proper imaging modalities such as computed tomography (CT) or magnetic resonance imaging (MRI) for performing accurate localization of tumors in that era, the treatments were only done for arteriovenous malformations (AVMs) at a dose rate of 30 Gy/min based on angiographic images.^[16,17]

In that era, SRS treatment was not limited to photon beams; simultaneous work on focused heavy particle irradiation



Figure 1: The first of two gamma knife units sold by Scanditronix under license from Elekta. It was manufactured by a subsidiary in Geneva called Nucletec. It came to Buenos Aires in 1983 and had a lot of problems which through various complications meant that Elekta could take back the license and then sell the first Gamma Knife in its own name to Pittsburgh in 1987. The second Nucletec version was sold to Sheffield in 1984 (Photo courtesy of ELEKTA)^[15]

was underway elsewhere. Ernest Lawrence, a professor at the University of California, Berkeley, created the cyclotron in 1929.^[9,17] Furthermore, Raymond Kjellberg at Harvard University was working on proton beams as well. Initially, in 1954, Lawrence irradiated the first patient with pituitary cancer but later continued his research with synchrotron and helium ions at Livermore laboratory, Berkeley.^[17]

In the 1980s, Winston and Lutz introduced a Brown-Roberts-Wells (BRW)-based system, that conventionally was used for stereotactic biopsy, to perform SRT using a Linac.^[18] Their quality assurance (QA) procedure, known as the “Winston-Lutz” test is still one of the major tests performed in clinics for Linac-based SRS treatments.^[18] Later in 1994, John Adler, who had taken a fellowship with Lars Leksell in 1985, treated the first patients with a CyberKnife [Figure 2].^[9,11] The CyberKnife (Accuray, Sunnyvale, CA, USA) is a robotic 6 MV Linac, equipped with live image guidance [Figure 3] to eliminate the need for invasive fixations and skull frames and could be used for the treatment of small tumors in different sites of the body.

In addition to enhancing the features and accuracy of the mentioned devices, some machines, like Vero (BrainLAB AG, Feldkirchen, Germany), were developed in the early 2010s. These machines are equipped with the ability to perform image-guided SBRT with non-coplanar rotation of the gantry, allowing for a greater degree of freedom in the treatment and coverage of tumors.^[12,19] In recent years, the Zap-X (ZAP Surgical Systems, San Carlos, California, USA) has been developed that is a self-contained, self-shielded therapeutic radiation device for the brain, as well as head-and-neck SRS. The Zap-X does not normally require a radiation bunker since it uses a 2.7 megavolt (MV) accelerating potential and incorporates radiation-shielded mechanical structures [Figure 4].^[13] The Zap-X utilizes an integrated planar kilovolt (kV) imaging system that spins around the patient’s head to provide three-dimensional (3D) patient registration.

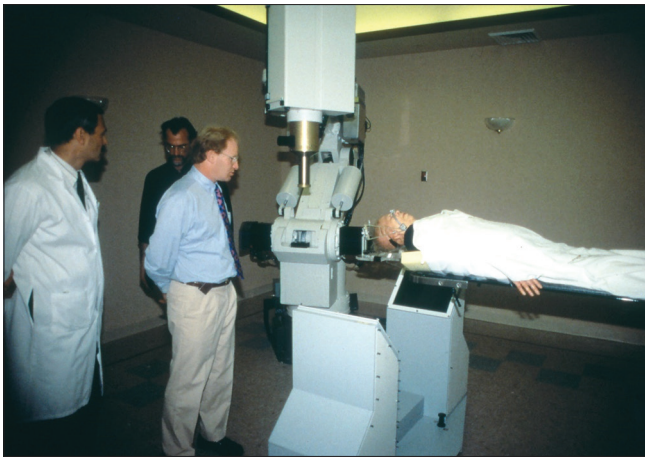


Figure 2: Dr. John Adler and the first patient treated with CyberKnife in 1994 (Photo courtesy of John R. Adler, MD)

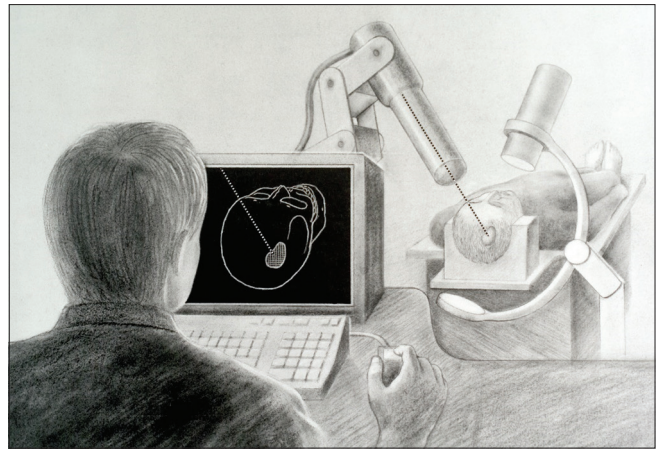


Figure 3: Early CyberKnife drawing equipped with a C-arm imager (Photo courtesy of John R. Adler, MD.)



Figure 4: Zap-X radiosurgery system (Photo courtesy of ZAP Surgical Systems)^[20]



Figure 5: The ICON, the latest model of Gamma Knife equipped with cone-beam computed tomography and gating (Photo courtesy of ELEKTA).

CyberKnife has evolved from a cone-shaped model to a 2.5 mm width micro-multi leaf collimator (MLC) model in the CyberKnife M6 version (since 2012) and later, CyberKnife S7 (2020), equipped with online tumor tracking.^[21] GK (AB Elekta, Stockholm, Sweden) has also progressed from the initial models U, B, and C to Perfexion, ICON, and Espirit models, which have the capability of collimator changes during treatment. The ICON model, which is equipped with pretreatment cone beam CT (CBCT) and optical motion management during treatment, no longer requires rigid radiosurgery frames [Figure 5]. On the other hand, Linac-based systems such as newer Varian (Siemens Healthineers AG, Frankfurt, Germany) products such as TrueBeam and Edge, in addition to CBCT and optical tracking, have a 2.5 mm width leaves in the center bank of the MLC, to shape the radiation field more accurately.^[22]

Nowadays, besides the SRS and SBRT-specific systems such as Gama Knife and CyberKnife, the majority of particle therapy and photon therapy modalities have the ability of stereotactic treatments. Along with this, accurate treatment planning, use of gating, and image guidance treatments have reduced complications and increased patient survival in some cases.^[23,24]

Table 1 provides an overview of significant developments in the field of SRS and radiotherapy over the years, highlighting key milestones and advancements.

TREATMENT PLANNING

Since MRI and CT, the most widely used imaging modalities in treatment planning and positioning, were invented in the years 1977^[25] and 1971,^[26] respectively, the first treatments by GK lacked accurate treatment planning. At that time, angiography or polytomography images were used to treat AVMs and acoustic neuromas, respectively.^[27]

In 1968, the dose distribution in a given area was estimated using manual summation of dose profiles from different directions of irradiation and transmitting on the radiographic image of the treatment areas.^[28] Therein, by calculating the effective radiological depth, the heterogeneities due to the air or bone were also considered. However, for GK, the first attempts to estimate the gamma-ray dose distribution were made in 1989.^[29] The year 1990 marked the introduction of a multi-isocenter method, which efficiently covered irregularly

Table 1: Significant developments in the field of stereotactic radiosurgery and radiotherapy over the years

Modality	Invention/ introduction year	Notable advancements	Energy
GK	1968	Evolved from orthovoltage X-rays to cobalt-60 sources	⁶⁰ Co gamma (1.17 and 1.33 MeV)
Linac-based radiosurgery	1980s	Noninvasive treatment, few fraction treatment	~6–15 MV
CyberKnife	1994	Transitioned to CyberKnife S7 with online tumor tracking	6 MV
Tomotherapy	2002	Introduced helical tomotherapy	6 MV
Vero	The early 2010s	Enabled image-guided SBRT with noncoplanar rotation	6 MV
Zap-X	Recent years	Self-contained, self-shielded device for brain SRS	3 MV

SRS: Stereotactic radiosurgery, SBRT: Stereotactic body radiation therapy, GK: Gamma Knife

shaped tumors by utilizing two or more radiation isocenters instead of one.^[30]

There are forward and inverse methods for treatment planning in radiotherapy. In forward treatment planning, first, the radiation beams are arranged in terms of energy, weight, shape, and direction, and after dose calculation by treatment planning system (TPS) and reviewing the results of dose distribution and dose volume histogram (DVH), changes are made by experienced treatment planners. In contrast, inverse treatment planning is now widely employed by most medical centers, utilizing computerized treatment planning with optimizing algorithms. By determining the dose objective/constraints of each organ at risk (OAR), clinical tumor volume (CTV), and planning target volume (PTV), the TPS algorithm is given the quantitative goal of treatment resulting in a plan optimized through iterative techniques. Depending on the TPS algorithm provided by the vendor as well as the treatment technique, the beam arrangement and the weight of each beam can be determined to meet the desired goals of treatment planning as much as possible.

Nowadays, with the advancement of imaging technology, image processing, and thanks to powerful computers, inverse planning has become the dominant planning technique in clinics. Image processing in treatment planning for SRS/SRT involves manipulating and analyzing medical images, using algorithms and automation, to enhance image quality, fuse different imaging modalities, and automating the segmentation of target volumes (TVs) and critical structures, leading to more efficient and precise treatment planning. These advancements streamline the process, improve accuracy, and contribute to standardized and optimized treatment outcomes in SRS/SRT. Several vendors offer Linac-based, CyberKnife, GK, Zap-X, or Tomotherapy TPSs with auto fusion and segmentation features. These include Varian Hyperarc,^[31] Brainlab Elements,^[32] Raysearch Raystation,^[33] and Elekta Monaco^[34] TPSs that support a volumetric modulated arc therapy (VMAT) or modality-specific dose calculations.

In 1998, inverse planning was used for treatment planning of complex tumors treated by CyberKnife.^[35,36] CyberKnife planning used singular values decomposition (SVD) to obtain the optimal minibeam weightings that allowed conformational dose distribution. SVD is a mathematical technique used in various fields, including image processing and radiation

therapy planning. In the context of radiation therapy planning, SVD is used for optimization and obtaining optimal minibeam weightings in TPSs such as CyberKnife. It is a matrix factorization method that decomposes a matrix into three components: U , Σ , and V . Given an $m \times n$ matrix A , where m represents the number of rows and n represents the number of columns, the SVD decomposition can be expressed as:^[37]

$$A = U\Sigma V^T \text{ Equation 1}$$

Here, U is an $m \times m$ orthogonal matrix, Σ is an $m \times n$ diagonal matrix with singular values arranged in descending order, and V^T is the transpose of an $n \times n$ orthogonal matrix. The singular values in Σ represent the importance of each mode of variation or component in matrix A .

In the case of CyberKnife treatment planning, SVD is employed to obtain the optimal minibeam weightings that allow for precise conformation of the dose distribution. These weightings play a crucial role in achieving the desired dose distribution for complex tumors treated with CyberKnife radiosurgery.

In the current state of treatment planning for SRS/SRT, there have also been advancements in the development of automated fusion and segmentation methods offered by various TPSs. These methods aim to streamline the process of combining multiple imaging modalities and accurately delineating TVs and critical structures. Auto-fusion techniques utilize algorithms and image registration methods to automatically align and fuse different imaging modalities, such as CT and MRI, for treatment planning.^[38] These methods help overcome the challenges of manual fusion, which can be time-consuming and prone to human error. By automating the fusion process, auto-fusion methods enhance efficiency and improve the accuracy of spatial alignment between different imaging datasets.

Similarly, auto-segmentation methods employ advanced algorithms, machine learning techniques, and atlas-based approaches to automatically outline and segment TVs and OARs based on the acquired imaging data. These methods reduce the reliance on manual contouring, which can be subjective and time-consuming, and provide consistent and reproducible segmentations. By accelerating the segmentation process, auto-segmentation methods contribute to increased efficiency and standardization in treatment planning.

It is important to consider that the performance of auto-fusion and auto-segmentation methods can vary depending on various factors. The accuracy of these methods is influenced by factors such as the specific algorithms used, the quality of the input imaging data, the complexity of the cases being treated, and the availability of accurate ground truth data for validation. Moreover, the accuracy of these methods should be evaluated on a case-by-case basis and validated against manual segmentation performed by experienced radiation oncologists. QA measures, including visual inspection and validation against ground truth data, are crucial to ensure the accuracy and reliability of both auto-fusion and auto-segmentation methods.

In CT-MR image registration, achieving an acceptable tolerance is critical for accurate target delineation and subsequent radiation dose delivery.^[39] The acceptable tolerance for CT-MR registration in SRS/SRT generally aims for submillimeter accuracy. However, it is important to strive for the highest possible accuracy to ensure precise target delineation and treatment planning. Advanced image registration techniques and QA processes, including visual inspection and quantitative validation, play key roles in achieving accurate CT-MR registration. The specific tolerance values may vary based on institutional guidelines, equipment capabilities, and the expertise of the treatment team. Regular quality control measures should be implemented to verify and maintain the accuracy of CT-MR registration throughout the treatment process.

Modern CT scanners offer high-resolution imaging capabilities, enabling detailed visualization of anatomical structures. These technological improvements have resulted in enhanced spatial resolution, improved image quality, and better delineation of TVs. With higher CT image resolution, there is increased accuracy in target localization and improved assessment of critical structures, ultimately leading to enhanced treatment precision and better patient outcomes.^[40]

Although the application of MRI as an imaging modality providing a better soft tissue contrast in comparison to CT for localizing the tumor began in the 1990s, it was not possible to use it as the principal image in treatment planning dose calculations.^[41,42] This limitation was due to the fact that MRI images, unlike CT, are not based on electron density and Hounsfield unit, but on the density of hydrogen. Electron densities are required for dose computation in photon therapy to account for heterogeneity corrections, as Compton scattering is the predominant interaction at therapeutic energies and depends on electron density. However, after applying distortion corrections and mathematical transformation a pseudo-CT image can be generated.^[43] This can eliminate the need for CT and MRI image fusion, and segmentations can be done directly on MR images.

Both 1.5 Tesla (T) and 3 Tesla (T) MRI scanners play crucial roles in SRS/SRT treatment planning, each with its own set of advantages and considerations.^[44] The 1.5 T MRI scanners are widely available and commonly used in clinical practice, making them more cost-effective compared to higher field strengths. They provide sufficient image quality for many SRS/

SRT applications and allow for adequate visualization of TVs and surrounding structures. However, they may have a lower signal-to-noise ratio, which can impact the visibility of fine anatomical details and limit the visualization of small lesions or challenging anatomical regions.

On the other hand, 3 T MRI scanners offer a higher signal-to-noise ratio, resulting in improved image quality and enhanced visualization of fine anatomical details.^[45] They exhibit increased sensitivity in detecting small lesions and subtle tissue changes. With better delineation of TVs and critical structures, 3 T MRI scanners contribute to improved treatment planning accuracy. However, they are associated with higher costs and limited availability compared to 1.5 T MRI. In addition, longer scan times can pose challenges for patients with limited tolerance for immobilization.

To delineate the treatment target, similar to other radiotherapy techniques, according to the International Commission on Radiation Units (ICRU) protocols^[46] gross tumor volume (GTV), CTV, internal tumor volume, and PTV are segmented. However, for brain radiosurgery cases, the GTV to CTV and CTV to PTV margins are usually as small as 0–1 mm and 0–2 mm, respectively.^[47] For other body sites with a higher probability of target movement, the CTV to PTV margin can be slightly larger, depending on the technique and treatment machine. For example, this margin for spinal radiosurgery is typically up to 3 mm.^[48] Moreover, the prescribed dose is inversely related to the size of the tumor. So that for radiosurgery of brain tumors smaller than 1 cm the prescribed dose may be as high as 22–25 Gy, but for larger tumors (2.5–3 cm) the prescribed dose is under 18 Gy.^[47,49] Depending on the treatment site, OARs are also contoured based on the Radiation Therapy Oncology Group (RTOG) recommendations and guidelines. These procedures are as common as other radiotherapy procedures.

The isodose coverage of PTV depends on the size, tumor site, and treatment technique. For brain metastasis radiosurgery by GK, the prescribed dose of 50% isodose covering the PTV is between 12–24 Gy, which means the maximum dose inside the PTV is 24–48 Gy.^[3,49] However, for CyberKnife and Linac-based techniques such as VMAT, the prescribed dose is 60%–80% isodoses. Due to the requirement of high dose conformity to a small-size tumor in SRS, while avoiding spillage of high-dose outside the PTV, ring dose optimization structures can be constructed around the PTV, either abutting the target or a little offset from the target's edge, as shown in Figure 6. Depending on the size and number of rings and their intervals, specific dose constraint values are assigned to them in the optimization stage of planning. This helps to limit high doses to outside of a PTV. Concentric rings can also be added to further define the dose gradient around the target. In the case of small cranial targets in SRS planning, it is common to see the dose fall to 50% of the prescribed dose within a distance of about 5 mm from the edge of the target. To optimize this dose conformity and dose gradient, a ring structure can be

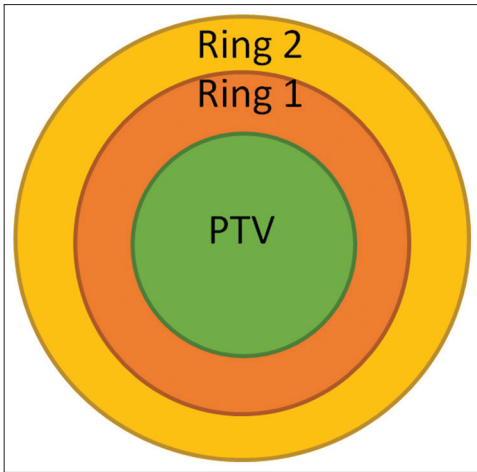


Figure 6: One of the methods used in SRS (and IMRT) to decrease the dose outside of the target. PTV and ring optimization structures used in SRS treatment planning to control dose fall off outside the target

added at a distance of 5 mm from the target edge with a limit of 50% of the prescribed dose. In conventional radiotherapy, however, the dose distribution is such that 95%–107% of the prescribed dose should cover PTV. Rings 1 and 2 in Figure 6 have a 5 mm width, with a dose constraint set to $D_{PTV} - 2\%$ and $D_{PTV}/2$, where D_{PTV} is the prescribed dose to PTV.^[50] For larger targets outside the skull, an intended ring can be larger and up to 2 cm from the edge of the PTV.^[50,51]

Compared to conventional radiation therapy, SRS uses smaller and more focused beams, resulting in a steep dose gradient and potentially worse dose homogeneity compared to conventional methods.^[52] This poses a higher risk of radiation-induced damage to surrounding healthy tissues, especially when the tumor is located near critical structures. However, the highly focused nature of SRS allows for higher doses to be delivered to the tumor while sparing surrounding healthy tissues, which can be beneficial in certain cases.

In 1993, the RTOG introduced a concept called conformity index (CI) to provide an estimate for dose coverage of PTV.^[53] The conformity index is the ratio of the volume that is covered by the prescribed dose to the TV [Figure 7]. It is also called the ratio of prescription isodose volume to TV. However, in the later years, newer concepts were added to reflect the dose to PTV and normal tissues simultaneously. van't Riet *et al.*^[54] and Paddick^[55] considered TV, the volume of the target covered by the reference isodose (TV_{RI}), and the volume of reference isodose line (V_{RI}) to define a more robust conformity index:

$$CN = \frac{TV_{RI}^2}{TV \times V_{RI}} \text{ Equation 2}$$

Moreover, a new conformity index (NCI) was defined to obtain a more accurate estimation of PTV coverage. Because CI provided a very general estimate of PTV coverage, it was not particularly effective for irregular shapes. The NCI is defined as follows:^[56]

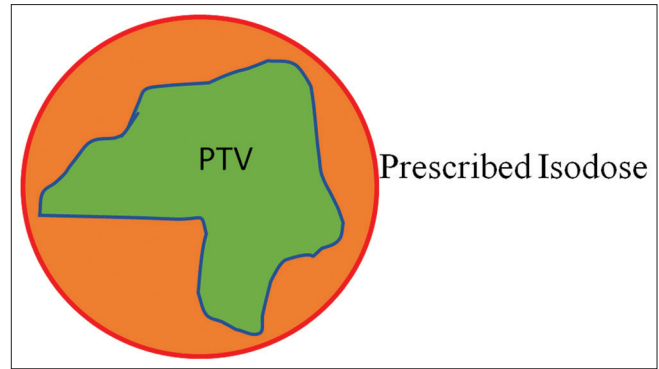


Figure 7: An example for conformity index (CI). The circle is an indication of the prescribed dose. Since the volume of the prescribed isodose is around twice the tumor volume, the CI is around 2 for this example

$$NCI = \frac{PV / TV_{PV}}{TV_{PV} / TV} \text{ Equation 3}$$

Where PV is the prescription volume, and TV_{PV} is the portion of the TV inside the prescribed isodose surface.

The Gradient Index^[57] is another quantitative measure used to evaluate the steepness or sharpness of the dose gradient at the edge of the TV. It provides an assessment of how quickly the dose drops off from the high-dose region to surrounding healthy tissues. A steeper dose gradient is desirable as it indicates better dose conformity, minimizing radiation to healthy tissues.

These indices, along with other metrics such as Homogeneity Index, Paddick Conformity Index,^[58] and Coverage Index,^[59] provide quantitative measures for evaluating the quality and effectiveness of SRS/SRT treatment plans. These metrics help radiation oncologists and physicists assess the dose distribution, target coverage, dose conformity, and dose homogeneity, ultimately guiding the optimization and refinement of treatment plans to achieve the desired treatment outcomes.

ICRU Report 91^[60] is essential in the context of SRS and SRT as it provides comprehensive guidelines for prescribing, recording, and reporting these treatments. These guidelines play a pivotal role in ensuring standardized and safe SRS/SRT procedures. They facilitate collaboration among healthcare professionals, including oncologists, physicists, and dosimetrists, who work together to optimize treatment plans using advanced planning systems. The recommendations in ICRU Report 91 assist in tailoring SRS/SRT treatments to individual patient needs, taking into account tumor characteristics, radiosensitivity, and normal tissue tolerance, ultimately maximizing treatment effectiveness while minimizing associated risks.

In recent years, some studies show that artificial intelligence (AI) may be able to assist in optimizing treatment planning for SRS and SBRT by analyzing large amounts of patient data, such as CT scans, MRI scans, and other imaging data, to help radiation oncologists determine the best treatment approach. AI algorithms can quickly process and analyze these data to generate optimized treatment plans, taking into account the

tumor location, size, shape, and proximity to critical organs, as well as the patient's individual characteristics, to deliver precise and personalized radiation therapy. AI can aid in accurate dose calculation for SRS and SBRT treatments. By leveraging machine learning algorithms, AI can help predict the radiation dose distribution within the tumor and surrounding healthy tissue, enabling radiation oncologists to optimize the treatment plan to achieve the desired therapeutic effect while minimizing the risk of side effects. Some studies and vendors are trying to employ AI in contouring and dose calculation of TPSs.^[61-63]

PATIENT POSITIONING

The importance of patient fixation during treatment, especially in a high-dose treatment, was considered from the very beginning of SRS because even small displacements and low uncertainties can lead to high doses of normal tissues. For these reasons, clinicians intended to achieve sub-millimeter accuracy from the beginning.^[64,65] Nowadays, the mechanical uncertainty of Linac-based SRS machines should have far less uncertainty than conventional radiotherapy (in most cases under 1 mm).^[66-68] For this reason, the frames that were originally used to fix the head were screwed directly to the skull to eliminate even the small movements caused by the displacement and compression of the skin.^[69] Figure 8 shows the first model of the Leksell stereotactic coordinate frame developed by Lars Leksell in 1949. He also developed other frames adapted to radiosurgery such as Model G, which is illustrated in Figure 9. This frame benefits from a 3D cartesian system to access the tumor for both neurosurgery and GK radiosurgery.

In 1974, the first commercial MRI was introduced by Electric and Musical Industries in London.^[70] Subsequently, to benefit from the contrast of MRI images, an MR-compatible fixation frame was developed by Dr. Leksell to be used for the GK machine, as illustrated in Figure 10.

Fixation systems such as BRW in 1979 increased the accuracy of CT-based SRS.^[71,72] This system was originally developed for neurosurgery and had a degree of freedom of access from all directions. The BRW frame was composed of a base ring and attached localizer rods. The average time to set up this frame was around 60 min.^[72] By marking the patient's head skin at three points and matching these points before imaging and before treatment, it was possible to increase the patient setup accuracy in Linac-based SRS.^[64,73] Moreover, the rods of the metal frame acted as fiducial markers in the images to provide more accurate localization of the tumor.

In the GK, a frame was attached to the skull bone by four pins. After fixing the frame and performing the imaging, which also required other accessories, the patient was ready for treatment. This setup enabled the placement of 3D Cartesian coordinates. The center of this system was actually the focal spot of tens of cobalt-60 sources. If one needed to treat two targets in the brain, the above process was done for each target separately.

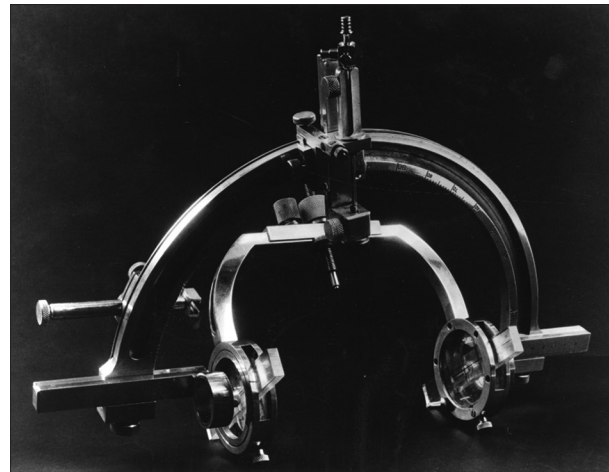


Figure 8: Leksell stereotactic radiosurgery coordinate frame developed by Lars Leksell in 1949 (Photo courtesy of ELEKTA)

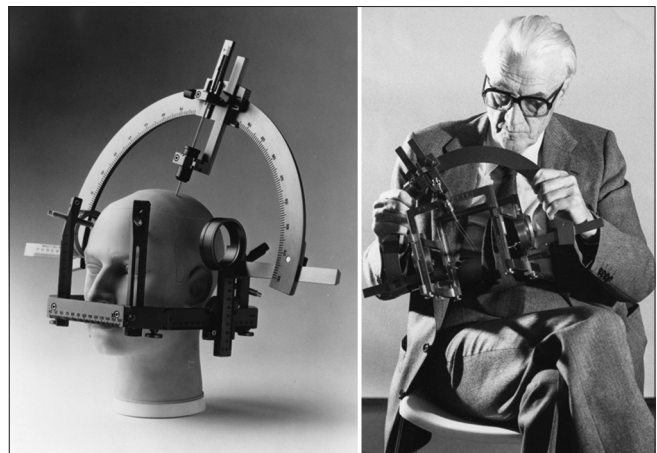


Figure 9: Leksell Coordinate Frame G, used for stereotactic neurosurgery and Gamma Knife radiosurgery (Photo courtesy of ELEKTA)

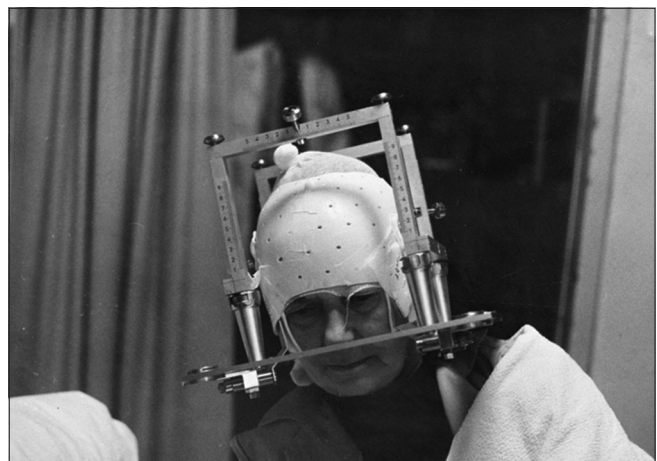


Figure 10: The plastic helmet in 1975 and modification that was made to work with Sweden's first magnetic resonance imaging scanner from Electric and Musical Industries (Photo courtesy of ELEKTA)

Finally, the frames were connected to the cobalt collimator's helmet through two pins.^[10] Currently, focal location and

adjustments are performed based on computer systems as well as CT and MR imaging.

In 1991, a patient-specific frame, the Gill-Thomas fixation system was introduced that was more convenient for patients in comparison to the previous invasive systems [Figure 11].^[74] In the first generations of Linac-based SRS, the frame was attached to the ground directly by a pedestal, instead of mounting it on the couch, to reduce frame displacement uncertainty,^[73] but this frame was placed on the couch, and fixed to the head by a bite block on the frame, and had an accuracy of a little more than 2 mm.^[75,76] As a result, it could not be used for single-fraction SRS, but it was accurate enough for the FSRT.

A few years later, with the introduction of CyberKnife and its frameless fixation, due to the image guidance system, the fixation of stereotactic radiation therapy entered a new phase. In later years, with the development of image-guided robotic radiosurgery, they were able to achieve accuracy of ± 0.3 and ± 1.0 mm for SBRT of the spine and pancreas, respectively.^[77] This image guidance was based on the tracking of bone landmarks in obtained X-ray images. However, in 1998 researchers from Japan introduced a monitoring device with nonionizing radiation for motion tracking through optical position measurement.^[78] They attached IR light emission diode markers on the head of patients to track their movements through a digital video camera. Therein, an excellent precision of <0.1 mm was reported.

Another system that was installed alongside Linacs in the early 2000s was the Novalis ExacTrac.^[79-82] Which has gone through its evolution over time. Initially, it was equipped with only two on-demand cross-sectional X-rays that could detect the patient body position in real-time. However, in newer versions, by optical tracking of the skin,^[83,84] it can include respiratory gating as well.

Gating the beam is a technique used during SBRT to reduce the risk of radiation exposure to normal tissues during treatment.

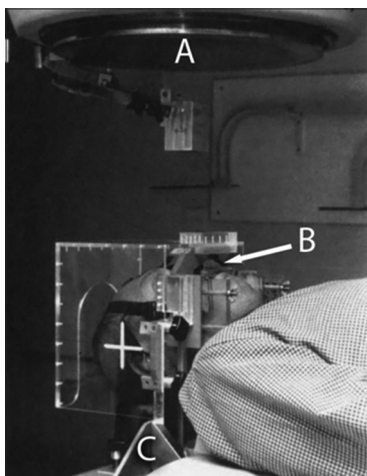


Figure 11: The GT fixation system for linear accelerator (Linac)-based stereotactic radiosurgery. (A) The linac head, (B) the biting device attached to the head frame, and (C) the frame stand fixed to the couch (image modified from ref^[74])

It involves synchronizing the delivery of the radiation beam with the patient's respiratory cycle, allowing the beam to be turned on only when the tumor is in the target area and avoiding radiation exposure to normal tissues during the breathing cycle. Gating the beam is achieved through the use of specialized imaging technology, such as CT or MRI, which can monitor the patient's breathing motion and provide real-time feedback to the radiation therapy machine. This allows the radiation beam to be adjusted and delivered with high precision, minimizing the risk of radiation exposure to normal tissues.

The idea of respiratory gating dates back to 1989.^[85] The system was based on the patient breathing into a bag, which changed the air pressure inside it. The beam was stopped and started according to the patient's inhale and exhale. Over time, gating throughout radiotherapy in general and SBRT in particular, has shifted to contactless methods including IR-based systems. The use of beam gating systems along with abdominal compression equipment and vacuum bags has greatly helped to reduce the uncertainty of SBRT treatment.

In addition to specialized companies such as Brainlab (BrainLAB, Heimstetten, Germany), Catalyst^[86] (C-RAD AB, Sweden), and Vision RT (Vision RT, London, UK),^[87] Linac manufacturers offer gating equipment, as an accessory to accelerators, including Clarity Autoscan^[88] system by Elekta company or RPM^[89] by Varian.

Recently, limited investigations have also been performed on the SRS and SBRT capability of some new combined modalities, such as MR-Linac,^[82-84] which integrate MRI with Linac technology. These cutting-edge systems offer real-time visualization of soft tissues and tumor motion during radiation delivery, allowing for improved target delineation and more precise radiation dose delivery. The early findings from these studies show promising results, indicating the potential of MR-Linac in enhancing the effectiveness and safety of SRS and SBRT treatments. As research in this field continues to evolve, further exploration of the clinical applications and long-term outcomes of MR-Linac for SRS and SBRT may uncover even more exciting possibilities in cancer treatment.^[90-92]

In modern linac setups, thermoplastic masks and vacuum cushions/bags are commonly used as immobilization devices. Thermoplastic masks are custom-fitted to the patient's face, head, or body and are secured to the treatment table, while vacuum cushions conform to the patient's body shape. These devices provide precise positioning and immobilization during treatment, and surface-guided radiation therapy (SGRT) plays a crucial role in SRS/SRT settings, utilizing camera systems to continuously monitor the patient's skin surface during treatment. SGRT ensures accurate setup, detects motion, allows for real-time repositioning, and facilitates adaptive radiotherapy, ultimately enhancing the precision and effectiveness of SRS/SRT treatments.^[93]

AI also can be utilized to enhance image-guided radiation therapy (IGRT), which involves using real-time imaging during treatment delivery to ensure accurate targeting of the tumor. Some studies show that AI algorithms can analyze the imaging data in realtime, track the tumor's position, and make necessary adjustments to the radiation delivery in response to changes in tumor position or patient anatomy, ensuring precise targeting of the tumor while sparing normal tissue.^[94]

QUALITY ASSURANCE

Due to the high dose per fraction and also the limited number of treatment fractions, any possible error or displacement in the radiation site can lead to irreparable damage to the patient and reduce the probability of therapeutic success.

In 1988, at the same time as introducing Linac-based SRS, Winston and Lutz introduced a test to measure the isocenter displacement.^[18,73] This famous test is still one of the mechanical QC tests for Linac-based SRS used today. They fixed a 4.8 mm steel ball at the isocenter on the patient's couch. A sheet of film attached to the gantry is irradiated at different gantry angles so that the back-projected image of the steel ball appears on the film. By measuring the deviation of the ball image on the film at different angles, the gantry error (mechanical and radiation isocenter coincidence) is determined. They also simulated tumor irradiation using a phantom head with nine steel bullets as a target simulator.

In the early 1990s, Bob Drzymala *et al.* published the results of their QA program.^[64,95] By introducing an irregular MR-compatible phantom, they compared the coincidence between the digitally reconstructed radiograph of the treatment planning and the treatment portal film. Moreover, using Arcs, they presented their daily QA program for maintaining the dose per each angle of gantry rotation. In 1995, the AAPM published TG42^[96] report on radiosurgery and QA. In this report, by expressing the equipment and facilities required to provide SRS treatment and stating the frequency of the tests, the average uncertainties that can be achieved in different parts of the SRS procedure, including CT imaging and frame placement were stated. They also described the QA for the treatment procedure of the patient couch of Linac-based, robotic, proton-based, and GK-based SRS, citing previous literature. The tests were mostly mechanical, and for target location controls, laser accuracy, patient couch, and stabilization frames. Most tests were based on Winston–Lutz and BRW.^[97]

In 2009, the AAPM TG 142 report,^[98] which was in fact an updated version of the TG40,^[65] dealt with the tolerances of various procedures including imaging, gantry, couch, and radiation field of Linacs. It also listed acceptable values for Linac-based SRS and SBRT. In that report, in most cases, the values of the device equipped with SRS or SBRT were more strict than similar machines that do not have these techniques. Most mechanical and MV or kV imaging tolerances were between 1 mm and 2 mm. While in TG40, no specific criteria were indicated for SRS (or SBRT) tolerances.

In 2010, AAPM TG 101^[68] for SBRT was released. The report referred to TG 40 and TG 142 for Linac-based SBRT accuracy testing. It was indicated that the multi-leaf collimator (MLC) with a width of 5 mm can be considered suitable for most cases. The dose calculation grid size is recommended to be 2 mm or smaller. Furthermore, due to the high dose per fraction and dose heterogeneity^[99] in SBRT, the use of bioeffect-based treatment planning such as an equivalent uniform dose EUD concept is recommended for considering the radiobiological effects of radiation on the OAR and tumor. Respiratory management, gating, IGRT, and optical tracking techniques are also recommended.

In 2017, joint guidelines of the AAPM and the Radiosurgery Society (RSS) covering the entire treatment process, commissioning, and QA were published.^[67] This AAPM guideline, which is under the category of the Medical Physics Practice Guideline (MPPG) group, was for the end-to-end testing process as well as mechanical and dosimetric tolerances of C-arm and robotic Linacs and helical Tomotherapy. Apart from this, in 2010 AAPM had also examined the QA of helical Tomotherapy in TG148.^[66]

AAPM's later report, TG 218^[100] in 2018, did not mention SRS or SBRT, but some articles discussed the possibility of employment of that report for SRS/SBRT QA purposes as well.^[101] The TG218 report considered the dose-tolerance action for IMRT and VMAT at a gamma index^[102] of 3%/2 mm. However, the guidelines^[101] suggested that depending on QA equipment, 3%/2 mm to 3%/1 mm could be used for SRS and SBRT. For multiple tumors, a strict value of 2%/1 mm was recommended.

New recommendations provide updated and comprehensive guidelines for the QA of GK treatments. They encompass a wide range of aspects, including treatment planning, dosimetry, image guidance, and patient-specific QA, tailored specifically to the unique characteristics of GK systems. Incorporating these recommendations into clinical practice ensures that GK Radiosurgery continues to deliver precise and effective treatments while minimizing the risk of errors. In addition to AAPM TG 178, other established QA protocols, such as those outlined by AAPM TG 142 and AAPM TG 101, continue to play crucial roles in the QA process for SRS and SRT across different modalities. These protocols address various aspects of treatment delivery, imaging, and patient safety, providing a comprehensive framework for QA.

For cobalt-based radiosurgery (GK), the QA protocols are also more limited due to the use of radioactive sources and fewer moving components than Linac-based machines. The first protocol, as mentioned earlier, was an RTOG^[53] protocol. However, AAPM TG 42 indicated the daily, monthly, and annual tests for GK. These tests include safety, physics, and dosimetry sections, mentioning the maximum recommended tolerances.

In terms of patient QA, various vendors have increased the quality of treatment by providing various testing equipment

such as detector arrays as well as cranial phantoms that can accommodate small detectors such as diodes. Efforts have always been made to bring the resolution of the array dosimeters closer to the films so that in addition to benefiting from the rapid analysis of dose distribution, the accuracy can be increased.

The Elekta's RTsafe,^[103] CIRS's STEEV,^[104] Standard Imaging's Lucy 3D QA,^[105] PTW's Ruby^[106] cranial phantoms, as well as high-resolution array detectors such as PTW's OCTAVIUS Detector 1600 SRS,^[107] Sun Nuclear's SRS MapCHECK,^[108] and IBA Dosimetry's myQA SRS^[109] are among the advanced equipment in this field. Some of these detector arrays also have an evaluation gamma index resolution of up to 2%/2 mm.

Failure Mode and Effects Analysis (FMEA)^[110] and TG 100^[111] are both proactive approaches that can be used to identify potential weak links in the QA chain for SRS. FMEA can be used to identify potential failure modes in the SRS process that could impact the quality of the treatment. This could include errors in the SRS planning or delivery process, such as incorrect patient positioning, inaccurate dosimetry calculations, or machine malfunction. By identifying these potential failure modes, steps can be taken to mitigate their impact or prevent them from occurring altogether. TG 100, on the other hand, provides a comprehensive set of guidelines and recommendations for all aspects of the SRS process, from patient simulation and imaging to treatment planning and delivery. Table 2 summarizes protocol developments in SRS and SRT.

Small-field dosimetry has undergone significant development over time in the field of QA. Advancements in detector technology, such as diode detectors and micro ionization chambers, have improved the accuracy and reliability of small field measurements. Correction factors for small field dosimetry have been refined and standardized, accounting

for effects such as volume averaging and lateral electronic disequilibrium.^[112,113] Monte Carlo simulations have played a crucial role in validating measurement techniques and optimizing treatment planning algorithms for SRS/SRT. Reference dosimetry protocols specifically tailored for small fields have been established, ensuring traceability and consistency in dose delivery.

Various detectors and measurement techniques play a vital role in QA processes for radiosurgery:

Ionization and solid state chambers

Ionization chambers are commonly used in radiosurgery QA to measure the dose delivered by the radiation beam accurately. These chambers provide precise and reliable measurements of radiation dose, helping ensure that the prescribed dose matches the delivered dose. They are often employed for reference dosimetry to calibrate the Linac or other radiosurgery equipment.

Diodes and solid-state detectors are also commonly used for radiation measurements. Diodes and solid-state detectors have advantages such as fast response times and small size, making them suitable for real-time dose verification. These detectors are integral to the chamber-based QA methods mentioned earlier.

Small field detectors play a crucial role in radiosurgery QA due to the precise and focused nature of the radiation beams used in these treatments. These detectors are typically characterized by their small active volumes, which are well-suited for measuring the radiation dose in the confined treatment fields of radiosurgery. Common small field detectors include:

Diodes

Diode detectors are among the most widely used small field detectors in radiosurgery QA. They are incredibly compact and have small active volumes, typically in the range of a

Table 2: Summary of the task group (American Association of Physicists in Medicine task group) reports and International Commission on Radiation Units reports related to radiosurgery practice guidelines and quality assurance

Name of task group or ICRU report	Year	Organization	Focus/purpose
AAPM TG 40	1994	AAPM	QA for linacs
AAPM TG 42	1995	AAPM	SRS
AAPM TG 142	2009	AAPM	QA for linacs
AAPM TG 101	2010	AAPM	Guidance for safe and effective SBRT practices
AAPM TG 148	2010	AAPM	QA for helical tomotherapy
AAPM TG 135	2011	AAPM	QA for robotic radiosurgery
AAPM TG 178	2021	AAPM	Guidelines for GK radiosurgery
ICRU 50	1993	ICRU	Prescribing, recording, and reporting photon beam therapy
ICRU 62	1999	ICRU	Prescribing, recording, and reporting photon beam therapy for breast cancer (supplement to ICRU 50)
ICRU 83	2010	ICRU	Prescribing, recording, and reporting IMRT
ICRU 93	2014	ICRU	Prescribing, recording, and reporting light ion beam therapy
ICRU 91	2019	ICRU	Prescribing, recording, and reporting of stereotactic treatments with small photon beams

AAPM TG: American Association of Physicists in Medicine task group, ICRU: International Commission on Radiation Units, QA: Quality assurance, IMRT: Intensity-modulated radiation therapy, SRS: Stereotactic radiosurgery, SBRT: Stereotactic body radiation therapy

few millimeters in diameter. Diodes provide excellent spatial resolution, making them suitable for measuring dose profiles in narrow beams.^[114]

Microdiamond detectors

Microdiamond detectors are another type of small field detector with an active volume on the order of micrometers. Their tiny size allows for high spatial resolution in dose measurements, making them particularly useful for radiosurgery QA, especially in the verification of small beam profiles and steep dose gradients.^[115]

Small chamber detectors

Small chamber detectors are specialized ionization chambers designed for measuring radiation doses in confined and small treatment fields. They have smaller sensitive volumes compared to conventional ionization chambers, making them well-suited for small-field dosimetry.^[116]

These detectors face unique challenges in small field measurements, including volume averaging effects, partial volume effects, and perturbations caused by the detector itself. Specialized correction factors and careful calibration procedures are often required to account for these challenges and ensure accurate dose measurements in small and highly focused radiation fields.

Gel dosimeters

Gel dosimeters are 3D radiation dosimeters that offer valuable insights into the dose distribution within the treatment volume. They are particularly useful for verifying complex treatment plans and assessing dose conformity. Gel dosimeters provide a visual representation of the dose distribution, allowing physicists and clinicians to evaluate treatment accuracy.^[117]

Gafchromic films

Gafchromic films are radiochromic films that change color in response to radiation exposure. These films are advantageous for radiosurgery QA due to their high spatial resolution and ease of use. Radiosurgery teams can use Gafchromic films to verify dose distributions, assess beam profiles, and validate treatment plans.^[118]

Detector arrays

Detector arrays, such as the Sun Nuclear SRS MapCHECK and PTW OCTAVIUS Detector 1600 SRS, which are mentioned above, consist of multiple small detectors arranged in a grid pattern. These arrays offer real-time dose verification and are particularly valuable for ensuring the accuracy of dynamic treatment techniques, including intensity-modulated radiosurgery.^[119,120]

Cranial phantoms

Cranial phantoms are anthropomorphic head-shaped objects equipped with detectors. These phantoms replicate the human anatomy and allow for comprehensive testing of the entire radiosurgery process, from patient setup to dose delivery. They are especially useful for end-to-end testing of treatment systems.^[121,122]

AI also may be used in SRS QA in the future to improve the accuracy and safety of the treatment. One possible application of AI in SRS QA is analyzing patient data, including treatment response and outcomes, to identify patterns and predict treatment outcomes. By monitoring patient data such as image scans, DVHs, and oncologist's reports during and after SRS and SBRT treatments, AI can assist in the early detection of treatment-related complications, evaluate treatment efficacy, and provide feedback to radiation oncologists for treatment modifications as needed.^[123,124]

Several studies provide evidence supporting the potential benefits of AI in SRS QA for radiation therapy. For example, a study^[125] demonstrated the effectiveness of AI algorithms in accurately segmenting targets and organs at risk in SRS treatment planning. This AI-based auto-segmentation reduced contouring time and improved the consistency and accuracy of target delineation, thereby enhancing treatment accuracy. In addition, a review study^[126] highlighted several studies demonstrating the use of AI in predicting treatment outcomes, optimizing treatment planning, and improving target delineation. These findings suggest that AI has the potential to enhance treatment accuracy, safety, and overall patient outcomes in radiation therapy. However, further research and validation are still needed to fully evaluate the benefits of AI in SRS QA and ensure its safe and effective integration into clinical practice.

RADIOBIOLOGY

In earlier years, SRS was focused on structures with functional disorders but nonmalignant anatomy, then on modifications of normal anatomy such as trigeminal neuralgia and AVMs, and finally on adenomas such as pituitary adenomas and meningiomas, and finally on cancer.^[127] As a result, at the beginning, the radiobiological concepts were not significant and also not very applicable. The concepts of radiobiology and fractionation became important over time. A contributing factor was also the low dose rate available of linacs at that time. Due to the low dose rate of Linacs, and the high dose per fraction of SRS, if a patient was treated with an accelerator in one fraction, they would have to be irradiated for up to several hours, so fractionation was proposed as a solution to shorten the treatment duration and make it technically possible. In addition, some types of malignancies, including vestibular schwannomas at the time, were basically treated by GK at a dose of 25 Gy in 5 days.^[9]

The most commonly used radiobiologic model for estimating the cell survival probability by radiation is the linear-quadratic (LQ) model that was proposed by Lea in the 1940s,^[128,129] as follows:

$$S = e^{-(\alpha D + \beta D^2)} \quad \text{Equation 4}$$

where the α and β are the indications of radiosensitivity of a specific cell type, and D is the prescribed dose. Although this

model has been questioned for very low and very high doses for *in vivo* experiments,^[130-132] it is still the most trusted model available.^[133]

In conventional radiotherapy, fractionation is used to reduce normal tissue complications.^[5] While dose per fraction up to 20 Gy is sufficiently compatible with the LQ model,^[134,135] observations have shown that tumor control results are better than those predicted by models such as LQ. These excellent results from SRS and SBRT are justified on the basis of tumor vascular damage.^[2,136-139] Otherwise, considering only the tumor control effects of radiation, the tumor should have been treated with doses of 80 to 90 Gy per single fraction,^[140] while SRS achieves the same tumor control with a maximum dose of 18-25 Gy.^[2] Moreover, to reduce the complications of normal tissues in SRS, the prescribed dose is usually reduced with the increasing size of the tumor. On the other hand, due to the reoxygenation effect^[141] larger tumors respond poorly to the same dose used for smaller tumors.^[142-144] As a result, control of larger tumors by SRS is less effective. This is one of the reasons why SRT and hypofractionated treatments have been taken into consideration, because the cells in the central parts of the tumor have more time to turn from hypoxic to oxalic and, consequently, be more radiosensitive.

To justify the reduction of normal tissue complications in SRT of larger tumors, a biologically effective dose (BED) can be obtained using the LQ model, which determines the effective dose, based on the radiosensitivity of the tissue as well as the dose per fraction:

$$\text{BED} = D \left(1 + \frac{d}{\alpha / \beta} \right) \text{ Equation 5}$$

where D is the prescribed dose, and d is the dose per fraction. For example, suppose a tumor with $\alpha/\beta=10$ Gy is surrounded by a normal tissue with $\alpha/\beta=3$ Gy. If this tumor is irradiated in a single 15 Gy fraction, the BED of the tumor and normal tissue will be 37.5 and 90 Gy, respectively. However, for a 5-fraction scheme, to maintain the tumor BED at the 37.5 Gy, the normal tissue BED is decreased to 66.6 Gy. This shows that the complication of normal tissue can be reduced in a fractionated regime compared to the single-fraction plan. With longer treatment time (usually more than 3–4 weeks) and depending on the type of tumor, a factor called tumor cell repopulation reduces BED. However, given that the number of SRT or hypofractionated SRS sessions never goes beyond 3 weeks, the negative effect of repopulation is not significant for SRT or SBRT.^[10,64-92]

CONCLUSION

The field of stereotaxy has evolved to encompass SRS and SRT, offering noninvasive alternatives for treating brain tumors and lesions. Various modalities and technologies, including GK, CyberKnife, VERO, Zap-X, and Linacs, have been developed to perform SRS and SRT. These techniques have advanced over time, aided by CT and MRI for improved

tumor localization. The benefits of SRS and SRT include reduced invasiveness, access to critical areas, treatment of multiple tumors, fewer side effects, and shorter treatment periods, ultimately improving patients' quality of life. However, there are ongoing challenges in the technical and clinical aspects of these techniques.

Furthermore, the role of AI in SRS and SRT holds potential for enhancing treatment accuracy, efficiency, and patient outcomes. AI can assist radiation oncologists in personalized treatment planning, dose calculation, real-time monitoring, outcome prediction, and decision support. Despite these advancements, it is worth noting that the manuscript lacks proper evidence to support the role of AI in the field.

It is important to acknowledge that while fast treatment delivery has been achieved through techniques such as FFF beam, significant improvements in treatment outcomes have not been observed. This raises questions about the effectiveness of high-dose rates in Linac-based systems.

In summary, SRS and SRT have revolutionized the field of stereotaxy, offering valuable treatment options for cranial lesions. The potential of AI in improving treatment outcomes is promising but requires further investigation. As the field continues to progress, advancements in Linac-based systems, such as higher dose rates and finer multileaf collimators, may enhance target coverage precision. In addition, the integration of combined treatment-diagnosis modalities, such as MR-Linac, holds the potential for providing accurate and noninvasive treatment while ensuring patient safety.

Financial support and sponsorship

Nil.

Conflicts of interest

There are no conflicts of interest.

REFERENCES

- Horsley V, Clarke RH. The structure and functions of the cerebellum examined by a new method. *Brain* 1908;31:45-124.
- Song CW, Kim MS, Cho LC, Dusenbery K, Speduto PW. Radiobiological basis of SBRT and SRS. *Int J Clin Oncol* 2014;19:570-8.
- Halasz LM, Rockhill JK. Stereotactic radiosurgery and stereotactic radiotherapy for brain metastases. *Surg Neurol Int* 2013;4:S185-91.
- Schmitt D, Blanck O, Gauer T, Fix MK, Brunner TB, Fleckenstein J, *et al.* Technological quality requirements for stereotactic radiotherapy: Expert review group consensus from the DGMP working group for physics and technology in stereotactic radiotherapy. *Strahlenther Onkol* 2020;196:421-43.
- Kirkpatrick JP, Soltys SG, Lo SS, Beal K, Shrieve DC, Brown PD. The radiosurgery fractionation quandary: Single fraction or hypofractionation? *Neuro Oncol* 2017;19:i38-49.
- Kocher M, Soffietti R, Abacioglu U, Villà S, Fauchon F, Baumert BG, *et al.* Adjuvant whole-brain radiotherapy versus observation after radiosurgery or surgical resection of one to three cerebral metastases: Results of the EORTC 22952-26001 study. *J Clin Oncol* 2011;29:134-41.
- Aoyama H, Tago M, Kato N, Toyoda T, Kenjyo M, Hirota S, *et al.* Neurocognitive function of patients with brain metastasis who received either whole brain radiotherapy plus stereotactic radiosurgery or radiosurgery alone. *Int J Radiat Oncol Biol Phys* 2007;68:1388-95.

8. Petti PL, Rivard MJ, Alvarez PE, Bednarz G, Daniel Bourland J, DeWerd LA, *et al.* Recommendations on the practice of calibration, dosimetry, and quality assurance for gamma stereotactic radiosurgery: Report of AAPM Task Group 178. *Med Phys* 2021;48:e733-70.
9. Schulder M, Patil V. The history of stereotactic radiosurgery. In: Chin LS, Regine WF, editors. *Principles and Practice of Stereotactic Radiosurgery*. New York, NY: Springer New York; 2008. p. 3-7.
10. Wu A, Lindner G, Maitz AH, Kalend AM, Lunsford LD, Flickinger JC, *et al.* Physics of gamma knife approach on convergent beams in stereotactic radiosurgery. *Int J Radiat Oncol Biol Phys* 1990;18:941-9.
11. Adler JR Jr, Chang SD, Murphy MJ, Doty J, Geis P, Hancock SL. The Cyberknife: A frameless robotic system for radiosurgery. *Stereotact Funct Neurosurg* 1997;69:124-8.
12. Depuydt T, Poels K, Verellen D, Engels B, Collen C, Buleteanu M, *et al.* Treating patients with real-time tumor tracking using the Vero gimbaled linac system: Implementation and first review. *Radiation Oncol* 2014;112:343-51.
13. Weidlich GA, Schneider MB, Simcic V, Oostman Z, Adler JR Jr. Self-shielding for the ZAP-X®: Revised characterization and evaluation. *Cureus* 2021;13:e13660.
14. Lunsford LD, Lars Leksell. Notes at the side of a raconteur. *Stereotact Funct Neurosurg* 1996;67:153-68.
15. Lozano AM, Gildenberg PL, Tasker RR. *Textbook of Stereotactic and Functional Neurosurgery*. Berlin, Heidelberg: Springer Science and Business Media; 2009.
16. Steiner L, Lindquist C, Adler JR, Torner JC, Alves W, Steiner M. Clinical outcome of radiosurgery for cerebral arteriovenous malformations. *J Neurosurg* 1992;77:1-8.
17. Lunsford LD, Niranjan A, Kano H, Kondziolka D. The technical evolution of gamma knife radiosurgery for arteriovenous malformations. *Prog Neurol Surg* 2013;27:22-34.
18. Winston KR, Lutz W. Linear accelerator as a neurosurgical tool for stereotactic radiosurgery. *Neurosurgery* 1988;22:454-64.
19. Solberg TD, Medin PM, Ramirez E, Ding C, Foster RD, Yordy J. Commissioning and initial stereotactic ablative radiotherapy experience with Vero. *J Appl Clin Med Phys* 2014;15:4685.
20. Center MN. Available from: <https://www.miamineurosciencecenter.com/en/services/zap-x-radiosurgery-system/>. [Last accessed on 2023 Sep 23].
21. McGuinness CM, Gottschalk AR, Lessard E, Nakamura JL, Pinnaduwa D, Pouliot J, *et al.* Investigating the clinical advantages of a robotic linac equipped with a multileaf collimator in the treatment of brain and prostate cancer patients. *J Appl Clin Med Phys* 2015;16:284-95.
22. Khaledi N, Hayes C, Belshaw L, Grattan M, Khan R, Gräfe JL. Treatment planning with a 2.5 MV photon beam for radiation therapy. *J Appl Clin Med Phys* 2022;23:e13811.
23. Claus EB, Horlacher A, Hsu L, Schwartz RB, Dello-Iacono D, Talos F, *et al.* Survival rates in patients with low-grade glioma after intraoperative magnetic resonance image guidance. *Cancer* 2005;103:1227-33.
24. Hsieh CH, Shueng PW, Wang LY, Huang YC, Liao LJ, Lo WC, *et al.* Impact of postoperative daily image-guided intensity-modulated radiotherapy on overall and local progression-free survival in patients with oral cavity cancer. *BMC Cancer* 2016;16:139.
25. Dawson MJ. *Paul Lauterbur and the Invention of MRI*. Cambridge, MA (U.S.A.): MIT Press; 2013.
26. Howell JD. The CT scan after 50 years – Continuity and change. *N Engl J Med* 2021;385:104-5.
27. Leksell L. Stereotactic radiosurgery. *J Neurol Neurosurg Psychiatry* 1983;46:797-803.
28. Laughlin JS. Realistic treatment planning. *Cancer* 1968;22:716-29.
29. Wu A, Kalend A, Malta A, Lunsford L, Flickinger J, Bloomer W. Dose distributions and treatment planning of leksell stereotactic gamma knife for radiosurgery. *Int J Radiat Oncol Biol Phys* 1989;17:196-7.
30. Flickinger JC, Lunsford LD, Wu A, Maitz AH, Kalend AM. Treatment planning for gamma knife radiosurgery with multiple isocenters. *Int J Radiat Oncol Biol Phys* 1990;18:1495-501.
31. Ruggieri R, Naccarato S, Mazzola R, Ricchetti F, Corradini S, Fiorentino A, *et al.* Linac-based VMAT radiosurgery for multiple brain lesions: comparison between a conventional multi-isocenter approach and a new dedicated mono-isocenter technique. *Radiat Oncol* 2018;13:38.
32. Saenz DL, Crownover R, Stathakis S, Papanikolaou N. A dosimetric analysis of a spine SBRT specific treatment planning system. *J Appl Clin Med Phys* 2019;20:154-9.
33. Bodensteiner D. RayStation: External beam treatment planning system. *Med Dosim* 2018;43:168-76.
34. Snyder JE, Hyer DE, Flynn RT, Boczkowski A, Wang D. The commissioning and validation of Monaco treatment planning system on an Elekta VersaHD linear accelerator. *J Appl Clin Med Phys* 2019;20:184-93.
35. Tombropoulos R, Latombe J, Adler J. *Inverse treatment planning for the CyberKnife*. Radiosurgery 1997. Vol. 2. Basel: Karger Publishers; 1998. p. 236-50.
36. Grandjean P, Platoni K, Lefkopoulos D, Merienne L, Schlienger M. Use of a general inverse technique for the conformational stereotactic treatment of complex intracranial lesions. *Int J Radiat Oncol Biol Phys* 1998;41:69-76.
37. Abdi H. Singular value decomposition (SVD) and generalized singular value decomposition. *Encyclopedia of measurement and statistics* 2007. 907-12.
38. Patro KC, Avinash A, Pradhan A, Tatineni S, Kundu C, Bhattacharyya PS, *et al.* Step by step stereotactic planning of meningioma: A guide to radiation oncologists – The ROSE case [radiation oncology from simulation to execution]. *J Curr Oncol* 2021;4:92.
39. Ramaseshan R, Heydarian M. Comprehensive quality assurance for stereotactic radiosurgery treatments. *Phys Med Biol* 2003;48:N199-205.
40. Lecchi M, Fossati P, Elisei F, Orecchia R, Lucignani G. Current concepts on imaging in radiotherapy. *Eur J Nucl Med Mol Imaging* 2008;35:821-37.
41. Flickinger JC, Lunsford LD, Kondziolka D, Maitz AH, Epstein AH, Simons SR, *et al.* Radiosurgery and brain tolerance: An analysis of neurodiagnostic imaging changes after gamma knife radiosurgery for arteriovenous malformations. *Int J Radiat Oncol Biol Phys* 1992;23:19-26.
42. Lindquist C. Gamma knife radiosurgery. *Semin Radiat Oncol* 1995;5:197-202. [doi: 10.1054/SRAO00500197].
43. Stanescu T, Jans HS, Pervez N, Stavrev P, Fallone BG. A study on the magnetic resonance imaging (MRI)-based radiation treatment planning of intracranial lesions. *Phys Med Biol* 2008;53:3579-93.
44. Mori Y, Nakazawa H, Hashizume C, Tsugawa T, Murai T. Dosimetric comparison of hypofractionated stereotactic radiotherapy by three different modalities for benign skull base tumors adjacent to functioning optic pathways. *Int J Radiat Res* 2019;17:519-30.
45. Khodarahmi I, Fritz J. The value of 3 tesla field strength for musculoskeletal magnetic resonance imaging. *Invest Radiol* 2021;56:749-63.
46. Units International Commission on Radiation Units and Measurements. ICRU Report 83 Prescribing, Recording, and Reporting Photon-beam Intensity-Modulated Radiation Therapy (IMRT). *Journal of the ICRU-Vol. 10 No 1* 2010. Oxford, UK: Oxford University Press; 2010.
47. Kocher M, Wittig A, Piroth MD, Treuer H, Seegenschmied H, Ruge M, *et al.* Stereotactic radiosurgery for treatment of brain metastases. A report of the DEGRO working group on stereotactic radiotherapy. *Strahlenther Onkol* 2014;190:521-32.
48. Cox BW, Spratt DE, Lovelock M, Bilsky MH, Lis E, Ryu S, *et al.* International spine radiosurgery consortium consensus guidelines for target volume definition in spinal stereotactic radiosurgery. *Int J Radiat Oncol Biol Phys* 2012;83:e597-605.
49. Shaw E, Scott C, Souhami L, Dinapoli R, Kline R, Loeffler J, *et al.* Single dose radiosurgical treatment of recurrent previously irradiated primary brain tumors and brain metastases: Final report of RTOG protocol 90-05. *Int J Radiat Oncol Biol Phys* 2000;47:291-8.
50. Lalonde RJ. Treatment planning for SRS and SBRT. In: *Stereotactic Radiosurgery and Stereotactic Body Radiation Therapy (SBRT)*. New York: Springer; 2018. p. 65.
51. Clark GM, Popple RA, Prendergast BM, Spencer SA, Thomas EM, Stewart JG, *et al.* Plan quality and treatment planning technique for

- single isocenter cranial radiosurgery with volumetric modulated arc therapy. *Pract Radiat Oncol* 2012;2:306-13.
52. Dahshan BA, Weir JS, Bice RP, Renz P, Cifarelli DT, Poplawski L, *et al.* Dose homogeneity analysis of adjuvant radiation treatment in surgically resected brain metastases: Comparison of IORT, SRS, and IMRT indices. *Brachytherapy* 2021;20:426-32.
 53. Shaw E, Kline R, Gillin M, Souhami L, Hirschfeld A, Dinapoli R, *et al.* Radiation Therapy Oncology Group: radiosurgery quality assurance guidelines. *Int J Radiat Oncol Biol Phys* 1993;27:1231-9.
 54. van't Riet A, Mak AC, Moerland MA, Elders LH, van der Zee W. A conformation number to quantify the degree of conformality in brachytherapy and external beam irradiation: application to the prostate. *Int J Radiat Oncol Biol Phys* 1997;37:731-6.
 55. Paddick I. A simple scoring ratio to index the conformity of radiosurgical treatment plans. Technical note. *J Neurosurg* 2000;93 Suppl 3:219-22.
 56. Nakamura JL, Verhey LJ, Smith V, Petti PL, Lamborn KR, Larson DA, *et al.* Dose conformity of gamma knife radiosurgery and risk factors for complications. *Int J Radiat Oncol Biol Phys* 2001;51:1313-9.
 57. Vergalaso I, Liu H, Alonso-Basanta M, Dong L, Li J, Nie K, *et al.* Multi-institutional dosimetric evaluation of modern day stereotactic radiosurgery (SRS) treatment options for multiple brain metastases. *Front Oncol* 2019;9:483.
 58. Paddick I, Lippitz B. A simple dose gradient measurement tool to complement the conformity index. *J Neurosurg* 2006;105:194-201.
 59. Bassalow R, Rodebaugh R. SU FF T 227: Evaluation of six dosimetric indices for cyber knife stereotactic radiosurgery treatment planning. *Med Phys* 2006;33 (6 Pt 10):2100.
 60. Wilke L, Andratschke N, Blanck O, Brunner TB, Combs SE, Grosu AL, *et al.* ICRU report 91 on prescribing, recording, and reporting of stereotactic treatments with small photon beams: Statement from the DEGRO/DGMP working group stereotactic radiotherapy and radiosurgery. *Strahlenther Onkol* 2019;195:193-8.
 61. Majumdar A, Allam N, Zabel WJ, Demidov V, Fluerau C, Vitkin IA. Binary dose level classification of tumour microvascular response to radiotherapy using artificial intelligence analysis of optical coherence tomography images. *Sci Rep* 2022;12:13995.
 62. Fukumitsu N, Nitta K, Terunuma T, Okumura T, Numajiri H, Oshiro Y, *et al.* Registration error of the liver CT using deformable image registration of MIM maestro and velocity AI. *BMC Med Imaging* 2017;17:30.
 63. Chamunyonga C, Edwards C, Caldwell P, Rutledge P, Burbury J. The impact of artificial intelligence and machine learning in radiation therapy: Considerations for future curriculum enhancement. *J Med Imaging Radiat Sci* 2020;51:214-20.
 64. Drzymala RE, Klein EE, Simpson JR, Rich KM, Wasserman TH, Purdy JA. Assurance of high quality linac-based stereotactic radiosurgery. *Int J Radiat Oncol Biol Phys* 1994;30:459-72.
 65. Kutcher GJ, Coia L, Gillin M, Hanson WF, Leibel S, Morton RJ, *et al.* Comprehensive QA for radiation oncology: Report of AAPM Radiation Therapy Committee Task Group 40. *Med Phys* 1994;21:581-618.
 66. Langen KM, Papanikolaou N, Balog J, Crilly R, Followill D, Goddu SM, *et al.* QA for helical tomotherapy: Report of the AAPM task group 148. *Med Phys* 2010;37:4817-53.
 67. Halvorsen PH, Cirino E, Das IJ, Garrett JA, Yang J, Yin FF, *et al.* AAPM-RSS medical physics practice guideline 9.a. For SRS-SBRT. *J Appl Clin Med Phys* 2017;18:10-21.
 68. Benedict SH, Yenice KM, Followill D, Galvin JM, Hinson W, Kavanagh B, *et al.* Stereotactic body radiation therapy: The report of AAPM task group 101. *Med Phys* 2010;37:4078-101.
 69. Fabrikant JI, Lyman JT, Hosobuchi Y. Stereotactic heavy-ion Bragg peak radiosurgery for intra-cranial vascular disorders: Method for treatment of deep arteriovenous malformations. *Br J Radiol* 1984;57:479-90.
 70. Nicolson M. Peter Mansfield, The long road to Stockholm: The story of magnetic resonance imaging: An autobiography (Oxford: Oxford University Press, 2013), pp. X, 241, £25.00, hardback, ISBN: 978-0-19-966454. *Med Hist* 2013;57:449-50.
 71. Brown RA. A stereotactic head frame for use with CT body scanners. *Invest Radiol* 1979;14:300-4.
 72. Apuzzo ML, Fredericks CA. The Brown-Roberts-Wells system. In: *Modern Stereotactic Neurosurgery*. Boston: Springer; 1988. p. 63-77.
 73. Lutz W, Winston KR, Maleki N. A system for stereotactic radiosurgery with a linear accelerator. *Int J Radiat Oncol Biol Phys* 1988;14:373-81.
 74. Gill SS, Thomas DG, Warrington AP, Brada M. Relocatable frame for stereotactic external beam radiotherapy. *Int J Radiat Oncol Biol Phys* 1991;20:599-603.
 75. Kooy HM, Dunbar SF, Tarbell NJ, Mannarino E, Ferarro N, Shusterman S, *et al.* Adaptation and verification of the relocatable Gill-Thomas-Cosman frame in stereotactic radiotherapy. *Int J Radiat Oncol Biol Phys* 1994;30:685-91.
 76. Das S, Isiah R, Rajesh B, Ravindran BP, Singh RR, Backianathan S, *et al.* Accuracy of relocation, evaluation of geometric uncertainties and clinical target volume (CTV) to planning target volume (PTV) margin in fractionated stereotactic radiotherapy for intracranial tumors using relocatable Gill-Thomas-Cosman (GTC) frame. *J Appl Clin Med Phys* 2010;12:3260.
 77. Chang S, Murphy M, Martin D, Hancock S, Doty J, Adler J. Image-guided robotic radiosurgery: Clinical and radiographic results with the CyberKnife. *Radiosurgery* 1999;3:23-33.
 78. Kai J, Shiomi H, Sasama T, Sato Y, Inoue T, Tamura S, *et al.* Optical high-precision three-dimensional position measurement system suitable for head motion tracking in frameless stereotactic radiosurgery. *Comput Aided Surg* 1998;3:257-63.
 79. Weiss E, Vorwerk H, Richter S, Hess CF. Interfractional and intrafractional accuracy during radiotherapy of gynecologic carcinomas: A comprehensive evaluation using the ExacTrac system. *Int J Radiat Oncol Biol Phys* 2003;56:69-79.
 80. Alheit H, Dornfeld S, Winkler C, Blank H, Geyer P. Stereotactic guided irradiation in prostatic cancer using the ExacTrac-system (BrainLab). *J Radiother Oncol* 2000;56 Suppl 1:107.
 81. Jin JY, Yin FF, Tenn SE, Medin PM, Solberg TD. Use of the BrainLAB ExacTrac X-Ray 6D system in image-guided radiotherapy. *Med Dosim* 2008;33:124-34.
 82. Lewis BC, Snyder WJ, Kim S, Kim T. Monitoring frequency of intra-fraction patient motion using the ExacTrac system for LINAC-based SRS treatments. *J Appl Clin Med Phys* 2018;19:58-63.
 83. Ippolito E, Fiore M, Di Donato A, Silipigni S, Rinaldi C, Cornacchione P, *et al.* Implementation of a voluntary deep inspiration breath hold technique (vDIBH) using BrainLab ExacTrac infrared optical tracking system. *PLoS One* 2018;13:e0195506.
 84. Levin-Epstein R, Qiao-Guan G, Juarez JE, Shen Z, Steinberg ML, Ruan D, *et al.* Clinical assessment of prostate displacement and planning target volume margins for stereotactic body radiotherapy of prostate cancer. *Front Oncol* 2020;10:539.
 85. Ohara K, Okumura T, Akisada M, Inada T, Mori T, Yokota H, *et al.* Irradiation synchronized with respiration gate. *Int J Radiat Oncol Biol Phys* 1989;17:853-7.
 86. Stieler F, Wenz F, Shi M, Lohr F. A novel surface imaging system for patient positioning and surveillance during radiotherapy. A phantom study and clinical evaluation. *Strahlenther Onkol* 2013;189:938-44.
 87. Waghorn B. Technical overview and features of the vision RT AlignRT® System. In: *Surface Guided Radiation Therapy*. Boca Raton: CRC Press; 2020. p. 95-116.
 88. Lachaine M, Falco T. Intrafractional prostate motion management with the clarity autoscans system. *Med Phys Int* 2013;1:72-80.
 89. Li XA, Stepaniak C, Gore E. Technical and dosimetric aspects of respiratory gating using a pressure-sensor motion monitoring system. *Med Phys* 2006;33:145-54.
 90. Boh Lim S, Tyagi N, Subashi E, Liang J, Chan M. An evaluation of the use of EBT-XD film for SRS/SBRT commissioning of a 1.5 Tesla MR-Linac system. *Phys Med* 2022;96:9-17.
 91. Dolan JL, Kim J, Snyder K, Chetty IJ, Wen N. Investigation of SRS spine treatment plan quality on a magnetic resonance image guided linear accelerator. *Cureus J Med Sci* 2019;11.
 92. Wen N, Kim J, Doemer A, Glide-Hurst C, Chetty IJ, Liu C, *et al.* Evaluation of a magnetic resonance guided linear accelerator for stereotactic radiosurgery treatment. *Radiother Oncol* 2018;127:460-6.

93. Hoisak JDP, Paxton AB, Waghorn BJ, Pawlicki T. Surface Guided Radiation Therapy. Boca Raton, FL: CRC Press; 2020.
94. Zhao W, Shen L, Islam MT, Qin W, Zhang Z, Liang X, et al. Artificial intelligence in image-guided radiotherapy: A review of treatment target localization. *Quant Imaging Med Surg* 2021;11:4881-94.
95. Drzymala RE, editor. Quality assurance for linac-based stereotactic radiosurgery. In: Proceedings of an American College of Medical Physics Symposium. Madison, WI: Medical Physics Publishing; 1991.
96. Schnell M, Bova F, Larson D, Leavitt D, Lutz W, Podgorsak E, et al. Stereotactic radiosurgery: The report of AAPM task group 42. *Med Phys* 1995;54:88.
97. Heilbrun MP, Roberts TS, Apuzzo ML, Wells TH Jr., Sabshin JK. Preliminary experience with Brown-Roberts-Wells (BRW) computerized tomography stereotaxic guidance system. *J Neurosurg* 1983;59:217-22.
98. Klein EE, Hanley J, Bayouth J, Yin FF, Simon W, Dresser S, et al. Task Group 142 report: Quality assurance of medical accelerators. *Med Phys* 2009;36:4197-212.
99. Kuperman VY, Lubich LM. Impact of target dose inhomogeneity on BED and EUD in lung SBRT. *Phys Med Biol* 2021;66:01NT02. Available from: <https://iopscience.iop.org/article/10.1088/1361-6560/abd0d1>. [Last accessed on 2023 Sep 23].
100. Miften M, Olch A, Mihailidis D, Moran J, Pawlicki T, Molineu A, et al. Tolerance limits and methodologies for IMRT measurement-based verification QA: Recommendations of AAPM Task Group No. 218. *Med Phys* 2018;45:e53-83.
101. Xia Y, Adamson J, Zlateva Y, Giles W. Application of TG-218 action limits to SRS and SBRT pre-treatment patient specific QA. *J Radiosurg SBRT* 2020;7:135-47.
102. Low DA, Harms WB, Mutic S, Purdy JA. A technique for the quantitative evaluation of dose distributions. *Med Phys* 1998;25:656-61.
103. Saenz DL, Li Y, Rasmussen K, Stathakis S, Pappas E, Papanikolaou N. Dosimetric and localization accuracy of Elekta high definition dynamic radiosurgery. *Phys Med* 2018;54:146-51.
104. Ambrose R, Presser J, editors. End-To-End testing of linac-based SRS using radiochromic film and CIRS STEEV phantom. In: Medical Physics. NJ USA: Wiley 111 River St, Hoboken; 2018.
105. Choi D, Gordon I, Ghebremedhin A, Wroe A, Schulte R, Bush D, et al. SU-E-T-268: Proton Radiosurgery End-To-End Testing Using Lucy 3D QA Phantom. *Medical Physics* 2014; 41:285.
106. Poppinga D, Kretschmer J, Brodbek L, Meyners J, Poppe B, Looe HK. Evaluation of the RUBY modular QA phantom for planar and non-coplanar VMAT and stereotactic radiations. *J Appl Clin Med Phys* 2020;21:69-79.
107. Blin A, Legavre J, Trifard E, Lefevre R, Lafond C, Bellec J. Evaluation of the Octavius 1600 SRS detector array for CyberKnife treatment plan verification. *Radiother Oncol* 2021;161:S1328.
108. Rose MS, Tirpak L, Van Casteren K, Zack J, Simon T, Schoenfeld A, et al. Multi-institution validation of a new high spatial resolution diode array for SRS and SBRT plan pretreatment quality assurance. *Med Phys* 2020;47:3153-64.
109. Stepanek C, Stapleton A, Haynes J, Fletcher S. PH-0323 clinical evaluation of the myQA SRS detector for stereotactic body radiotherapy plan verification. *Radiother Oncol* 2021;161:S233-5.
110. Stamatis DH. Failure Mode and Effect Analysis: FMEA from Theory to Execution. Milwaukee, Wisconsin: Quality Press; 2003.
111. Huq MS, Fraass BA, Dunscombe PB, Gibbons JP Jr., Ibbott GS, Mundt AJ, et al. The report of task group 100 of the AAPM: Application of risk analysis methods to radiation therapy quality management. *Med Phys* 2016;43:4209.
112. Carrasco P, Jornet N, Duch MA, Weber L, Ginjaume M, Eudaldo T, et al. Comparison of dose calculation algorithms in phantoms with lung equivalent heterogeneities under conditions of lateral electronic disequilibrium. *Med Phys* 2004;31:2899-911.
113. International Atomic Energy Agency. Dosimetry of Small Static Fields Used in External Beam Radiotherapy. Vienna: International Atomic Energy Agency; 2017.
114. Pantelis E, Niroomand-Rad A. Use of radiochromic films in commissioning and quality assurance of CyberKnife®. In: Radiochromic Film: Role and Applications in Radiation Dosimetry. Milwaukee, Wisconsin: CRC Press; 2017. p. 203-26.
115. Shaw M, Lye J, Alves A, Keehan S, Lehmann J, Hanlon M, et al. Characterisation of a synthetic diamond detector for end-to-end dosimetry in stereotactic body radiotherapy and radiosurgery. *Phys Imaging Radiat Oncol* 2021;20:40-5.
116. Qin Y, Gardner SJ, Kim J, Huang Y, Wen N, Doemer A, et al. Technical Note: Evaluation of plastic scintillator detector for small field stereotactic patient-specific quality assurance. *Med Phys* 2017;44:5509-16.
117. Kudrevicius L, Jaselske E, Adliene D, Rudzianskas V, Radziunas A, Tamasauskas A. Application of 3D gel dosimetry as a quality assurance tool in functional Leksell gamma knife radiosurgery. *Gels* 2022;8:69.
118. Wen N, Lu S, Kim J, Qin Y, Huang Y, Zhao B, et al. Precise film dosimetry for stereotactic radiosurgery and stereotactic body radiotherapy quality assurance using Gafchromic™ EBT3 films. *Radiat Oncol* 2016;11:132.
119. Yasui K, Saito Y, Ogawa S, Hayashi N. Dosimetric characterization of a new two-dimensional diode detector array used for stereotactic radiosurgery quality assurance. *Int J Radiat Res* 2021;19:281-9.
120. Lin MH, Veltchev I, Koren S, Ma C, Li J. Robotic radiosurgery system patient-specific QA for extracranial treatments using the planar ion chamber array and the cylindrical diode array. *J Appl Clin Med Phys* 2015;16:290-305.
121. Dimitriadis A, Palmer AL, Thomas RAS, Nisbet A, Clark CH. Adaptation and validation of a commercial head phantom for cranial radiosurgery dosimetry end-to-end audit. *Br J Radiol* 2017;90:1-9.
122. Dieterich S. Quality assurance of image-guidance for pediatric patients in frameless stereotactic radiosurgery. *Int J Radiat Oncol Biol Phys* 2010;78:S786.
123. Appelt AL, Elhaminia B, Gooya A, Gilbert A, Nix M. Deep learning for radiotherapy outcome prediction using dose data – A review. *Clin Oncol (R Coll Radiol)* 2022;34:e87-96.
124. Chan MF, Witztum A, Valdes G. Integration of AI and machine learning in radiotherapy QA. *Front Artif Intell* 2020;3:577620.
125. Elguindi S, Zelefsky MJ, Jiang J, Veeraraghavan H, Deasy JO, Hunt MA, et al. Deep learning-based auto-segmentation of targets and organs-at-risk for magnetic resonance imaging only planning of prostate radiotherapy. *Phys Imaging Radiat Oncol* 2019;12:80-6.
126. Parkinson C, Matthams C, Foley K, Spezi E. Artificial intelligence in radiation oncology: A review of its current status and potential application for the radiotherapy workforce. *Radiography (Lond)* 2021;27 Suppl 1:S63-8.
127. Rosenthal DI, Glatstein E. We've got a treatment, but what's the disease? Or a brief history of hypofractionation and its relationship to stereotactic radiosurgery. *Oncologist* 1996;1:1-7.
128. Mitchell J. Actions of radiations on living cells. *Nature* 1946;158:601-2. [doi.org/10.1038/158601a0].
129. Lea D, Catcheside D. The mechanism of the induction by radiation of chromosome aberrations in *Tradescantia*. *J Genet* 1942;44:216-45.
130. Glatstein E. The omega on alpha and beta. *Int J Radiat Oncol Biol Phys* 2011;81:319-20.
131. Chapman JD, Gillespie CJ. The power of radiation biophysics-let's use it. *Int J Radiat Oncol Biol Phys* 2012;84:309-11.
132. Brenner DJ, Sachs RK, Peters LJ, Withers HR, Hall EJ. We forget at our peril the lessons built into the α/β model. *Int J Radiat Oncol Biol Phys* 2012;82:1312-4.
133. McMahon SJ. The linear quadratic model: Usage, interpretation and challenges. *Phys Med Biol* 2018;64:1-24.
134. Brenner DJ, editor. The linear-quadratic model is an appropriate methodology for determining isoeffective doses at large doses per fraction. In: Seminars in Radiation Oncology. United Kingdom: Elsevier; 2008.
135. Guerrero M, Li XA. Extending the linear-quadratic model for large fraction doses pertinent to stereotactic radiotherapy. *Phys Med Biol* 2004;49:4825-35.
136. Lasnitzki I. A quantitative analysis of the direct and indirect action of X radiation on malignant cells. *Br J Radiol* 1947;20:240-7.

137. Clement JJ, Song CW, Levitt SH. Changes in functional vascularity and cell number following x-irradiation of a murine carcinoma. *Int J Radiat Oncol Biol Phys* 1976;1:671-8.
138. Song CW, Cho LC, Yuan J, Dusenbery KE, Griffin RJ, Levitt SH. Radiobiology of stereotactic body radiation therapy/stereotactic radiosurgery and the linear-quadratic model. *Int J Radiat Oncol Biol Phys* 2013;87:18-9.
139. Song CW, Glatstein E, Marks LB, Emami B, Grimm J, Sperduto PW, *et al.* Biological principles of stereotactic body radiation therapy (SBRT) and stereotactic radiation surgery (SRS): Indirect cell death. *Int J Radiat Oncol Biol Phys* 2021;110:21-34.
140. Leith JT, Cook S, Chougule P, Calabresi P, Wahlberg L, Lindquist C, *et al.* Intrinsic and extrinsic characteristics of human tumors relevant to radiosurgery: Comparative cellular radiosensitivity and hypoxic percentages. *Acta Neurochir Suppl* 1994;62:18-27.
141. Clement JJ, Tanaka N, Song CW. Tumor reoxygenation and postirradiation vascular changes. *Radiology* 1978;127:799-803.
142. Solberg TD, Selch MT, Smathers JB, DeSalles AA. Fractionated stereotactic radiotherapy: Rationale and methods. *Med Dosim* 1998;23:209-19.
143. Vogelbaum MA, Angelov L, Lee SY, Li L, Barnett GH, Suh JH. Local control of brain metastases by stereotactic radiosurgery in relation to dose to the tumor margin. *J Neurosurg* 2006;104:907-12.
144. Khaledi N, Hayes C, Belshaw L, Grattan M, Khan R, Grafe JL. Treatment planning with a 2.5 MV photon beam for radiation therapy. *J Appl Clin Med Phys*. 2022; 23:e13811. [doi: 10.1002/acm2.13811].